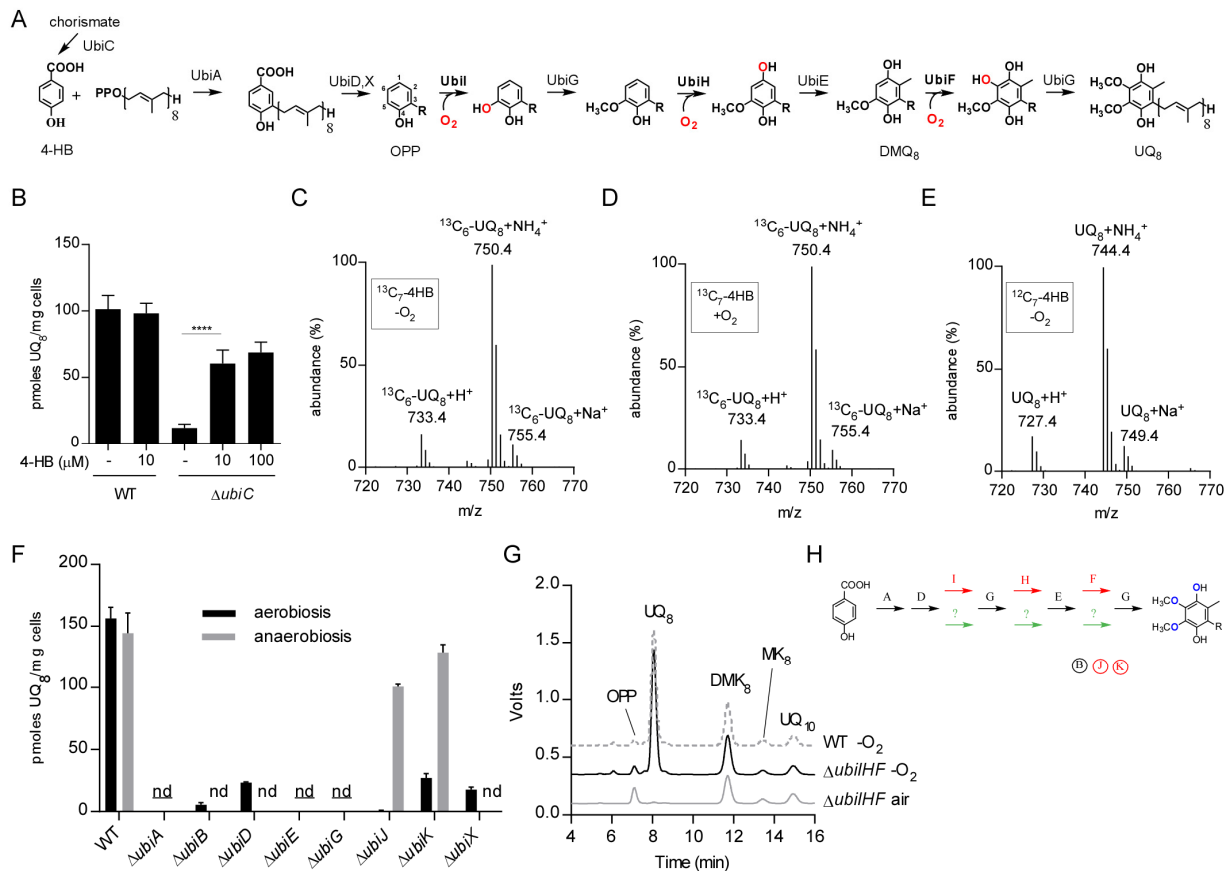


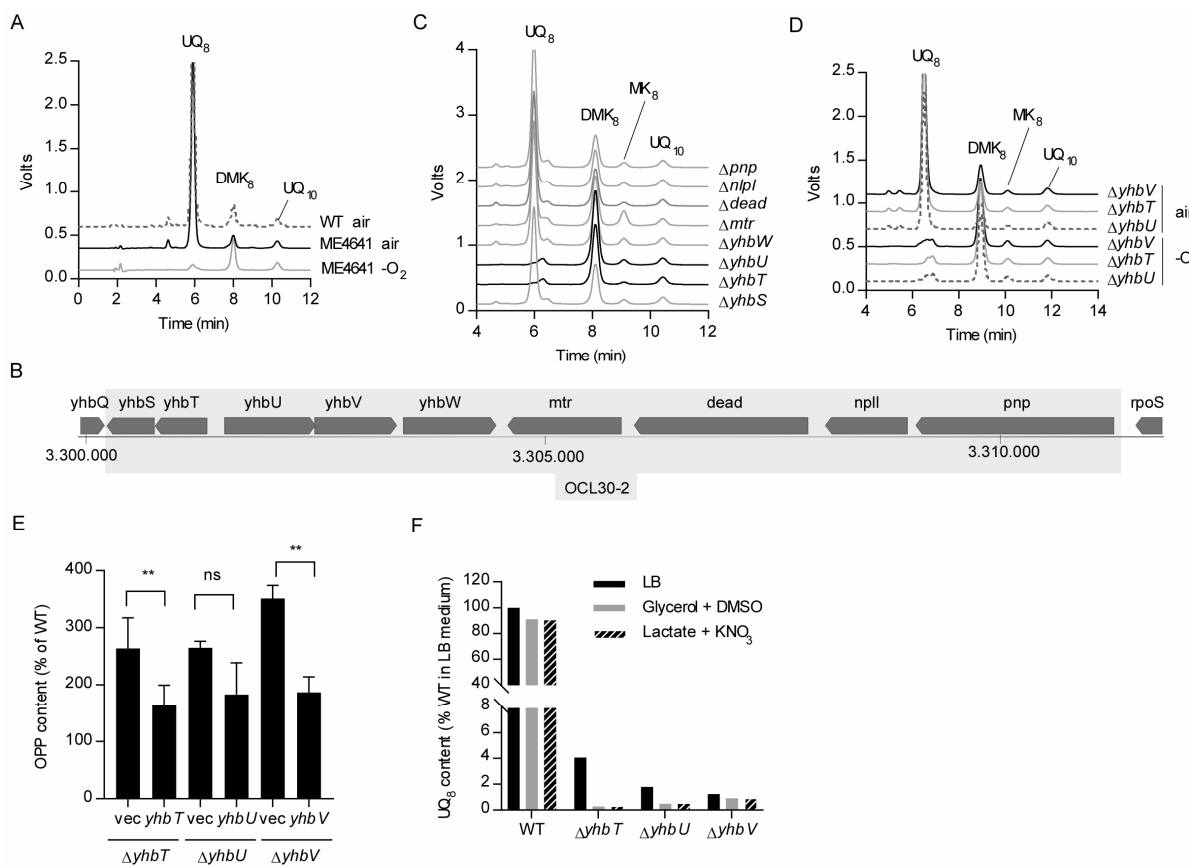
819 MAIN FIGURES

820



821

Figure 1: The aerobic and anaerobic UQ biosynthetic pathways differ only in the hydroxylation steps. A) O₂-dependent UQ biosynthesis pathway in *E. coli*. The octaprenyl tail is represented by R on the biosynthetic intermediates and the numbering of the aromatic carbon atoms is shown on OPP. Abbreviations used are 4-HB for 4-hydroxybenzoic acid, OPP for octaprenylphenol, DMQ₈ for C6-demethoxy-ubiquinone 8 and UQ₈ for ubiquinone 8. B) UQ₈ quantification of WT and Δ ubiC cells grown anaerobically in glycerol-nitrate medium supplemented or not with the indicated concentrations of 4-HB (n=3-6), ***: p<0.0001, unpaired Student's t test. C-E) Mass spectra of UQ₈ obtained by HPLC-MS analysis of lipid extracts from cells grown with ¹³C-4HB either anaerobically (C) or aerobically (D), or anaerobically with unlabeled 4HB (E). F) UQ₈ quantification from WT and Δ ubi cells grown anaerobically in SMGN medium overnight or aerobically in LB medium until OD 0.8. nd = not detected in aerobic and anaerobic conditions, nd= not detected in either aerobic or anaerobic conditions, n=3-4. G) HPLC-ECD analyses (mobile phase 1) of lipid extracts from 1 mg of WT or Δ ubilHF cells grown in LB medium in air or anaerobic conditions (-O₂). Chromatograms are representative of n=3 independent experiments (UQ₁₀ used as standard). H) UQ biosynthesis represented with Ubi enzymes specific to the O₂-dependent pathway (red), to the O₂-independent pathway (green), or common to both pathways (black). The same color code applies to the accessory factors (circled).

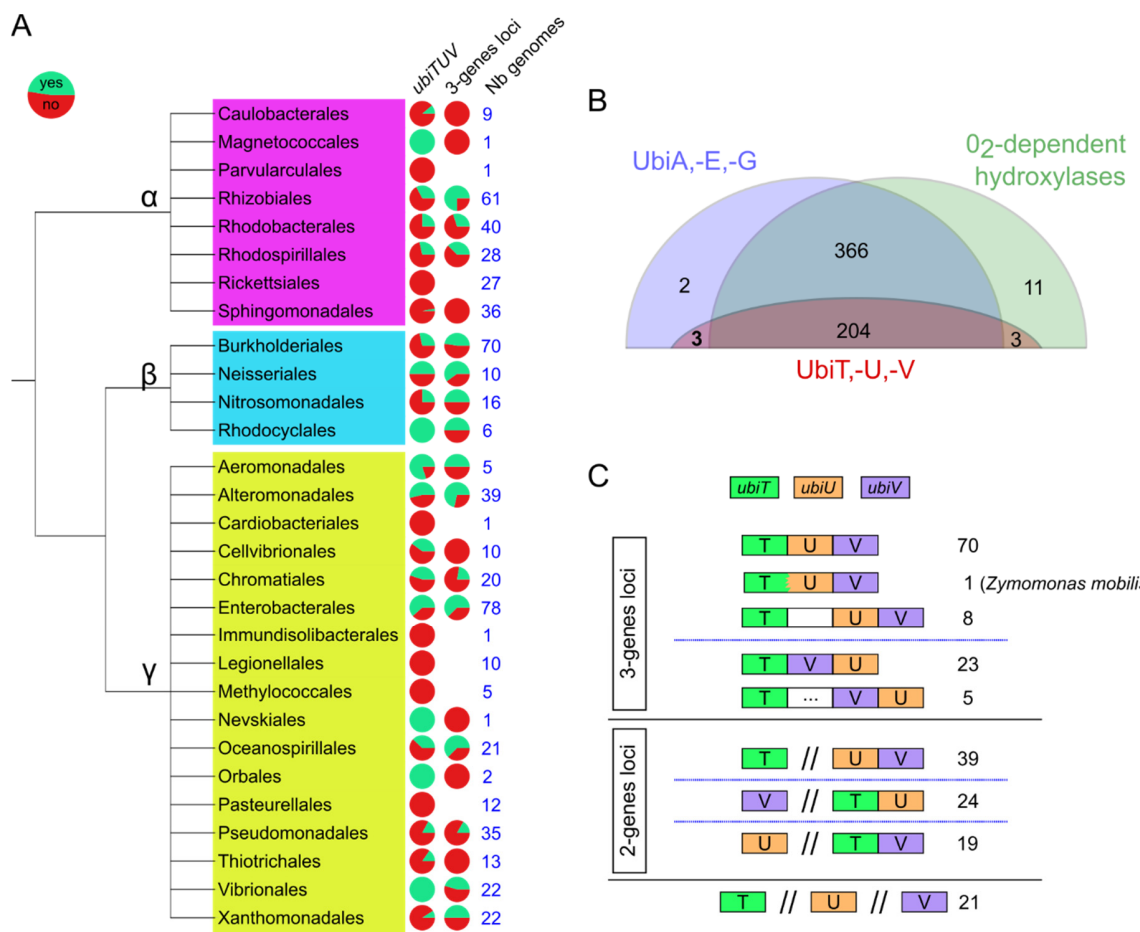


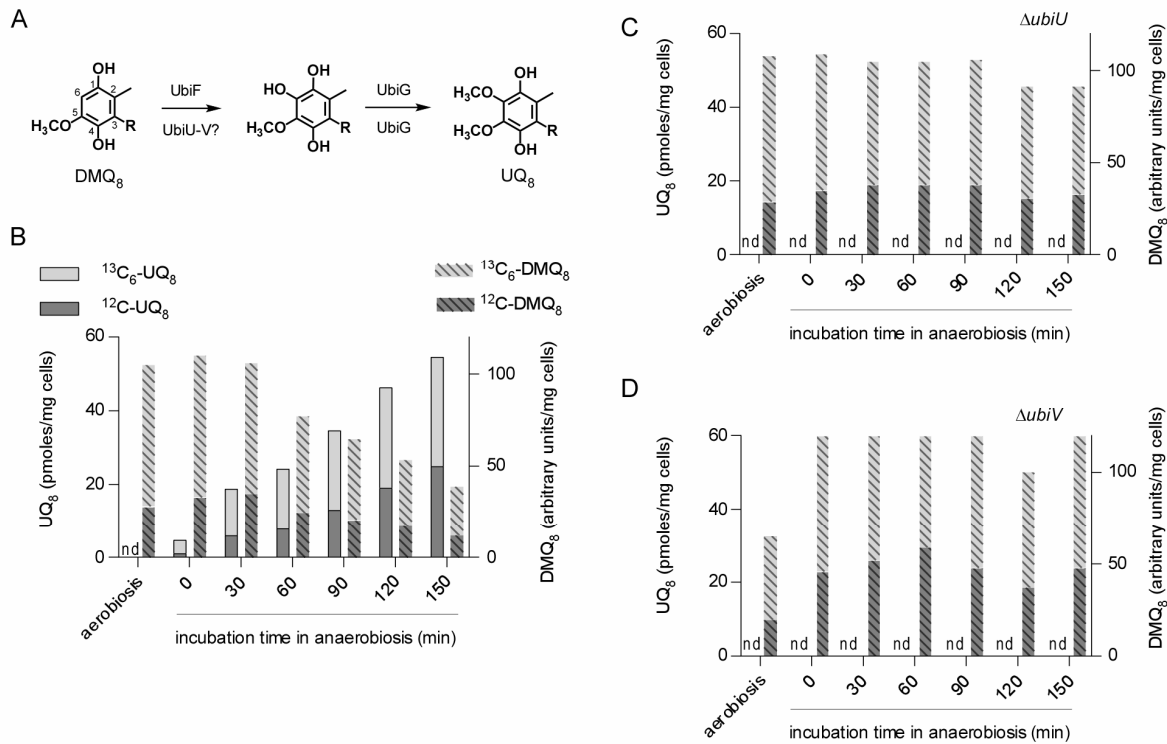
838

839

840 **Figure 2: *yhbT*, *yhbU* and *yhbV* are essential to the anaerobic biosynthesis of UQ.** A) HPLC-ECD analysis
 841 of lipid extracts from ME4641 strain grown in SMGN either aerobically or anaerobically (-O₂). B) Genomic
 842 region covered by the OCL30-2 deletion in the ME4641 strain. C) HPLC-ECD analysis of lipid extracts from
 843 knock-out strains of the individual genes covered by the OCL30-2 deletion grown in SMGN anaerobically.
 844 D) HPLC-ECD analysis of lipid extracts from $\Delta yhbT$, $\Delta yhbU$ and $\Delta yhbV$ strains constructed in the MG1655
 845 background and grown in glycerol nitrate medium either aerobically or anaerobically. HPLC-ECD analyses
 846 with mobile phase 2 (A, C, D). E) OPP content (as % of WT, mass detection M+NH₄⁺) in cells from table 2.
 847 The Δyhb strains contain either an empty plasmid or a plasmid carrying the indicated gene and were
 848 cultured anaerobically in glycerol nitrate medium containing 0.02% arabinose. mean \pm SD (n=3-5), **: p<
 849 0.01, unpaired Student's t test. F) UQ₈ content (as % of WT grown in LB medium) of cells cultured
 850 anaerobically in SM containing the indicated carbon sources and electron acceptors.

851



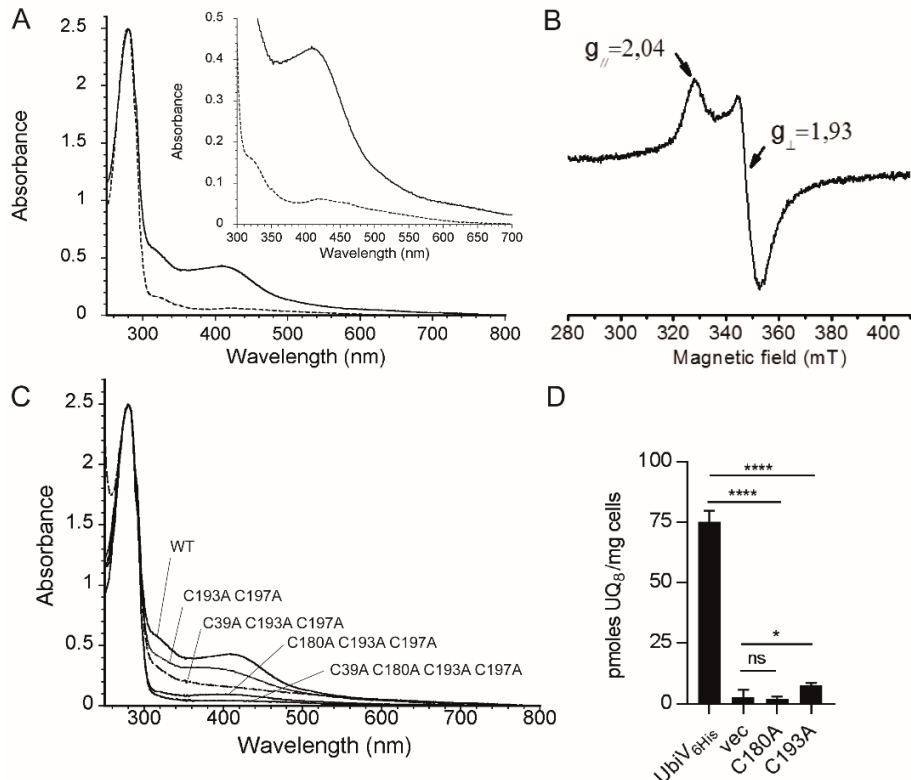


867

868 **Figure 4: UbiU and UbiV are necessary for the anaerobic conversion of DMQ₈ into UQ₈.** A) Conversion of
 869 DMQ₈ to UQ₈ with enzymes of the O₂-dependent and the O₂-independent pathways, indicated respectively
 870 above and below arrows (numbering of carbon atoms shown on DMQ₈ and polypropenyl tail represented by
 871 R). B) Unlabeled (¹²C) and labeled (¹³C₆) -DMQ₈ and -UQ₈ contents in ΔubiC ΔubiF cells after aerobic growth
 872 and transition to anaerobiosis. C-D) Same as in B with ΔubiC ΔubiF ΔubiU cells (C) and ΔubiC ΔubiF ΔubiV
 873 cells (D). nd, not detected, results representative of two independent experiments (B-D).

874

875

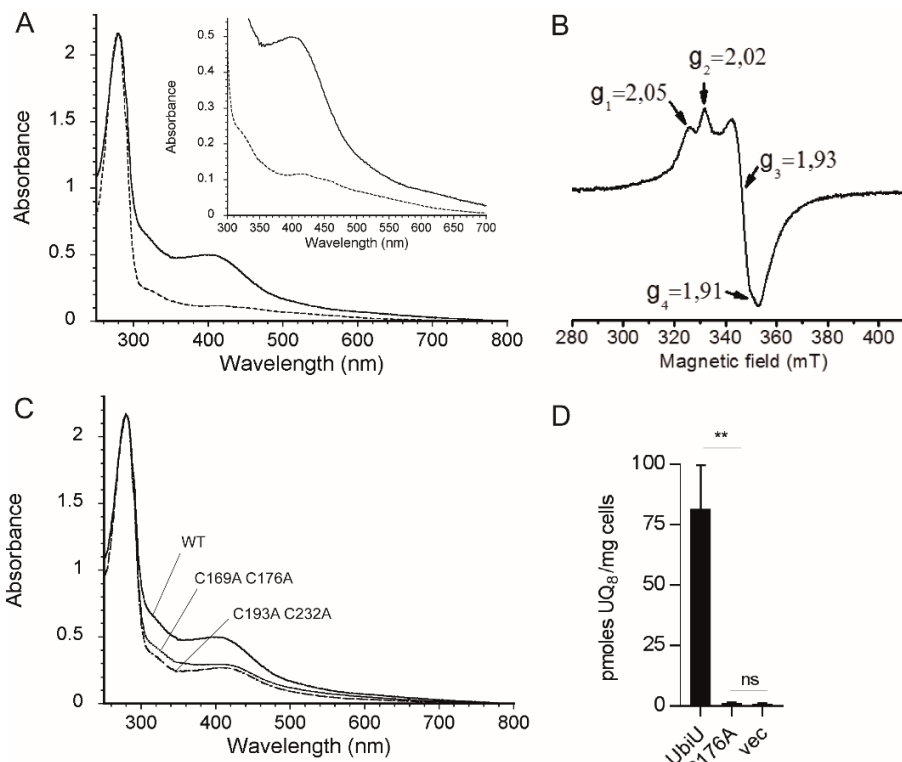


876

877 **Figure 5: UbiV binds a [4Fe-4S] cluster.** A) UV-visible absorption spectra of as-purified UbiV (dotted line,
878 47 μ M) and reconstituted holo-UbiV (solid line, 41 μ M); Inset: enlargement of the 300-700 nm region. The
879 molar extinction coefficient $\epsilon_{410\text{nm}}$ was determined to be $10.8 \pm 0.4 \text{ mM}^{-1} \text{ cm}^{-1}$ for holo-UbiV. B) X-band EPR
880 spectrum of 785 μ M dithionite-reduced holo-UbiV. Recording conditions: temperature, 10K; microwave
881 power, 10 mW; modulation amplitude, 0.6 mT. C) Comparative UV-visible absorption spectra of WT and
882 different Cys-to-Ala mutants of UbiV after metal cluster reconstitution, with the following concentrations:
883 41 μ M WT, 44 μ M C193A C197A, 46 μ M C39A C193A C197A, 47 μ M C180A C193A C197A, and 54 μ M C39A
884 C180A C193A C197A. Proteins were in 50 mM Tris-HCl, pH 8.5, 25 mM NaCl, 15% glycerol, 1m M DTT (A-
885 C). D) UQ₈ quantification of $\Delta ubiV$ cells transformed with pBAD-UbiV_{6His}, pBAD-UbiV_{6His} C180A, pBAD-
886 UbiV_{6His} C193A or empty pBAD and grown overnight in anaerobic MSGN (n=4-5). Mean \pm SD, *: p < 0.05,
887 ***: p < 0.0001, unpaired Student's t test.

888

889



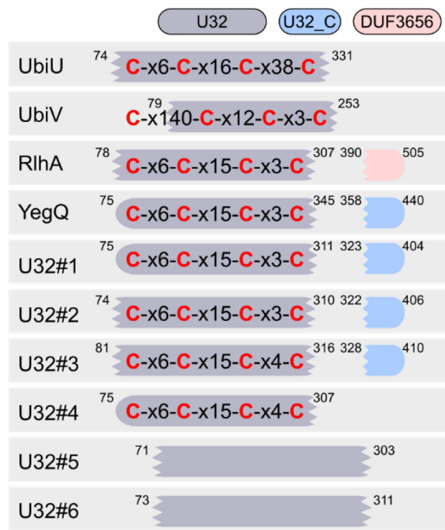
890

891

892 **Figure 6: The UbiU-V complex binds two [4Fe-4S] clusters.** A) UV-visible absorption spectra of as-purified
 893 UbiU-UbiV (dotted line, 17 μ M) and reconstituted holo-UbiU-UbiV (solid line, 15.5 μ M); Inset: enlargement
 894 of the 300-700 nm region. B) X-band EPR spectrum of 339 μ M dithionite-reduced holo-UbiU-UbiV;
 895 Recording conditions: temperature, 10K; microwave power, 2 mW; modulation amplitude, 0.6 mT. C)
 896 Comparative UV-visible absorption spectra of Cys-to-Ala mutants of UbiU in the UbiU-UbiV complex after
 897 metal cluster reconstitution with the following concentrations: 15.5 μ M WT, 16.0 μ M UbiU-C169A C176A
 898 and 16.0 μ M UbiU-C193A C232A. Proteins were in 50mM Tris-HCl, pH 8.5, 150mM NaCl, 15% glycerol and
 899 1mM DTT (A-C). D) UQ₈ quantification of Δ ubiU cells transformed with pBAD-UbiU (n=4), pBAD-UbiU
 900 C176A (n=2) or pBAD empty vector (n=3) and grown overnight in anaerobic MSGN. mean \pm SD, **: p< 0.01,
 901 ns: not significant, unpaired Student's t test.

902

903



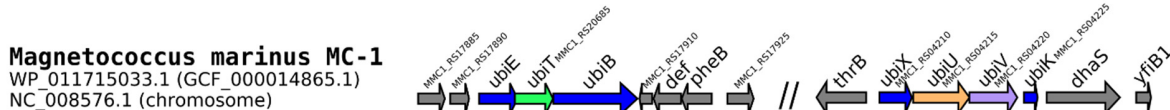
904

Figure 7: Conserved four cysteines motifs in the U32 protease family.

905 The conserved 4-cysteines motifs and PFAM domains (colored boxes) found in each U32 protease family
 906 are displayed for a set of reference sequences. These motifs were obtained by aligning the sequences
 907 listed by Kimura *et al.* [42]. Conserved cysteines are in red, "x6" indicates that 6 residues were found in
 908 between two conserved cysteines. Positions of the domains are displayed on the outside of the boxes for
 909 the reference sequences. Scrambled extremities show interrupted match for the PFAM domain. No
 910 conserved cysteines were found for U32#5 and U32#6 (see main text). Reference sequences were from *E.*
 911 *coli* for UbiU, UbiV, YegQ and RhA (YHBU_ECOLI, YHBV_ECOLI, YEGQ_ECOLI, YDCP_ECOLI for RhA). For
 912 the rest of the families, the sequence accession numbers were: R7JPV1_9FIRM for U32#1, R6XKQ3_9CLOT
 913 for U32#2, S1NZZ5_9ENTE for U32#3, H1YXA1_9EURY for U32#4, H3NJ45_9LACT for U32#5,
 914 D5MIQ1_9BACT for U32#6.

915 SUPPLEMENTARY FIGURES

916



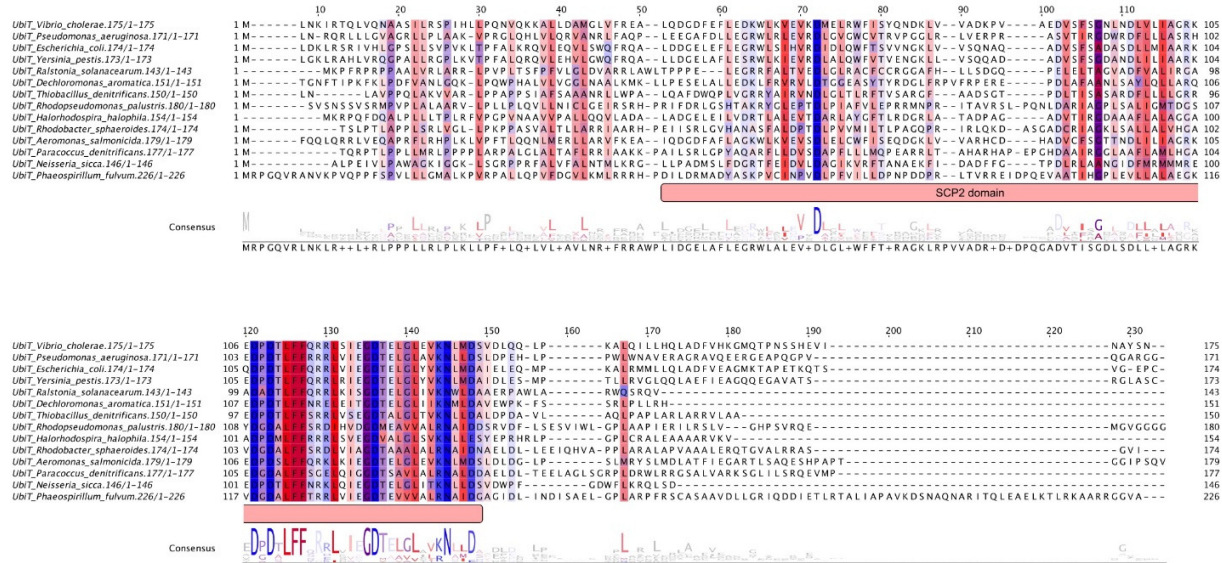
917

Figure S1: Genetic context of the *ubiT,U,V* genes in *M. marinus*. The scheme was drawn from a figure obtained using the GeneSpy program [77].

920

921

922



923

924 **Figure S2:** Multiple sequence alignment of UbiT from representative proteobacteria. Sequences were
 925 aligned using Mafft (linsi), and the output generated using Jalview and Inkscape. Hydrophobic residues are
 926 colored in blue. The position of the SCP2 domain (PF02036) is indicated by a red box. Genbank accession
 927 numbers: *Vibrio cholerae*, NP_230303.1, *Pseudomonas aeruginosa*, NP_252600.1, *Escherichia coli*,
 928 NP_312065.1, *Yersinia pestis*, YP_002348366.1, *Ralstonia solanacearum*, WP_011004260.1,
 929 *Dechloromonas aromaticata*, WP_011285876.1, *Thiobacillus denitrificans*, WP_011312695.1,
 930 *Rhodopseudomonas palustris*, WP_011666115.1, *Halorhodospira halophila*, WP_011813831.1,
 931 *Rhodobacter sphaeroides*, WP_011909347.1, *Aeromonas salmonicida*, WP_005310396.1, *Paracoccus*
 932 *denitrificans*, WP_011750456.1, *Neisseria sicca*, WP_080614297.1, *Phaeospirillum fulvum*,
 933 WP_074767212.1.

934

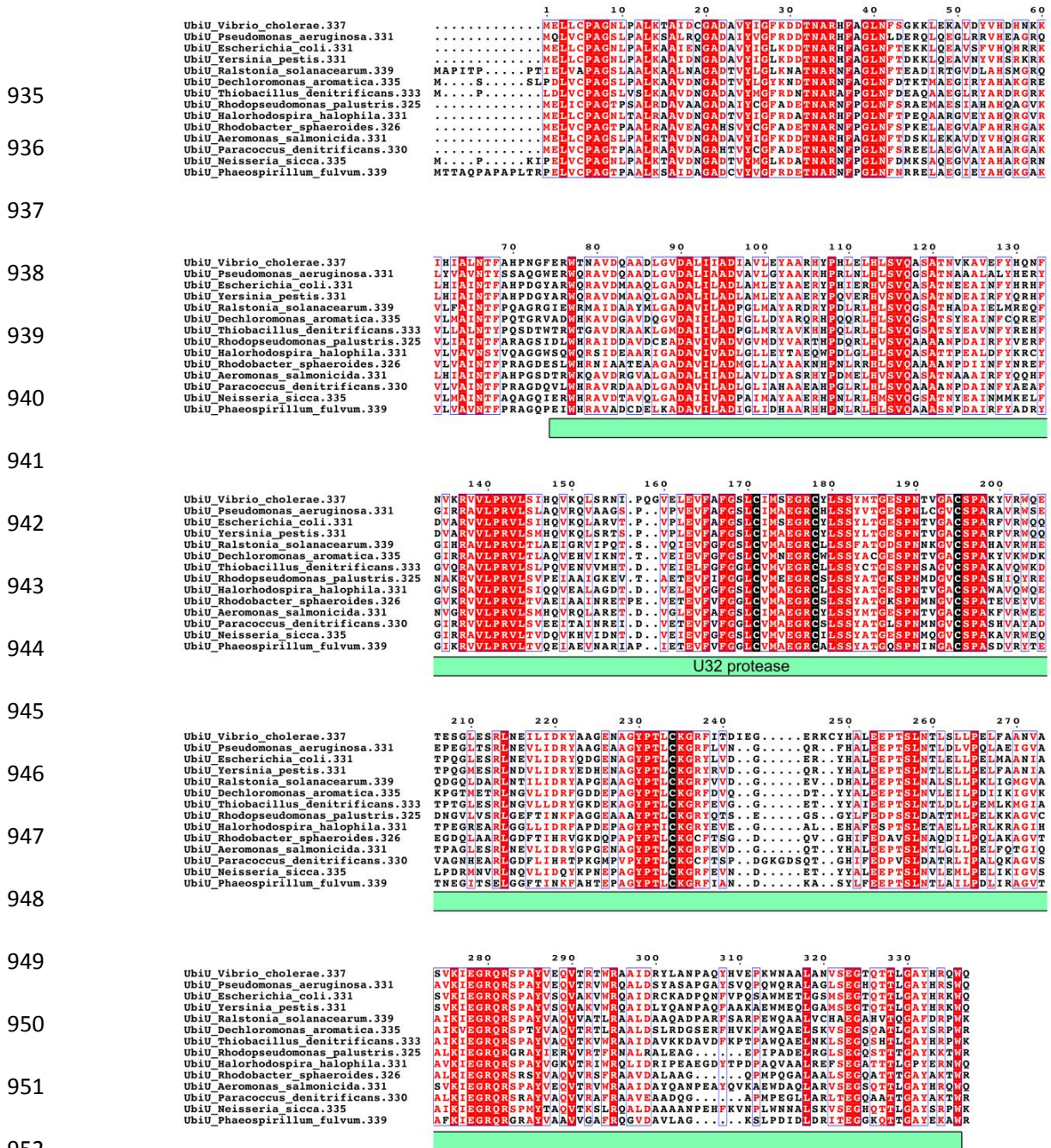


Figure S3: Multiple sequence alignment of UbiU from representative proteobacteria. Sequences were aligned using Mafft (linsi), and the output generated using ESPript and Inkscape. The four conserved cysteines (C169, C176, C193 and C232) involved in iron-sulfur binding are indicated by black columns. The position of the domain U32 protease PF01136 is indicated by a green box. GenBank accession numbers: *Vibrio cholerae*, NP_230301.1, *Pseudomonas aeruginosa*, NP_252602.1, *Escherichia coli*, NP_312066.1, *Yersinia pestis*, YP_002348368.1, *Ralstonia solanacearum*, WP_011004262.1, *Dechloromonas aromaticana*, WP_011285878.1, *Thiobacillus denitrificans*, WP_011312698.1, *Rhodopseudomonas palustris*, WP_011666114.1, *Halorhodospira halophila*, WP_011813833.1, *Rhodobacter sphaeroides*, WP_011909346.1, *Aeromonas salmonicida*, WP_005310394.1, *Paracoccus denitrificans*, WP_041530457.1, *Neisseria sicca*, WP_049226489.1, *Phaeospirillum fulvum*, WP_074767209.1.

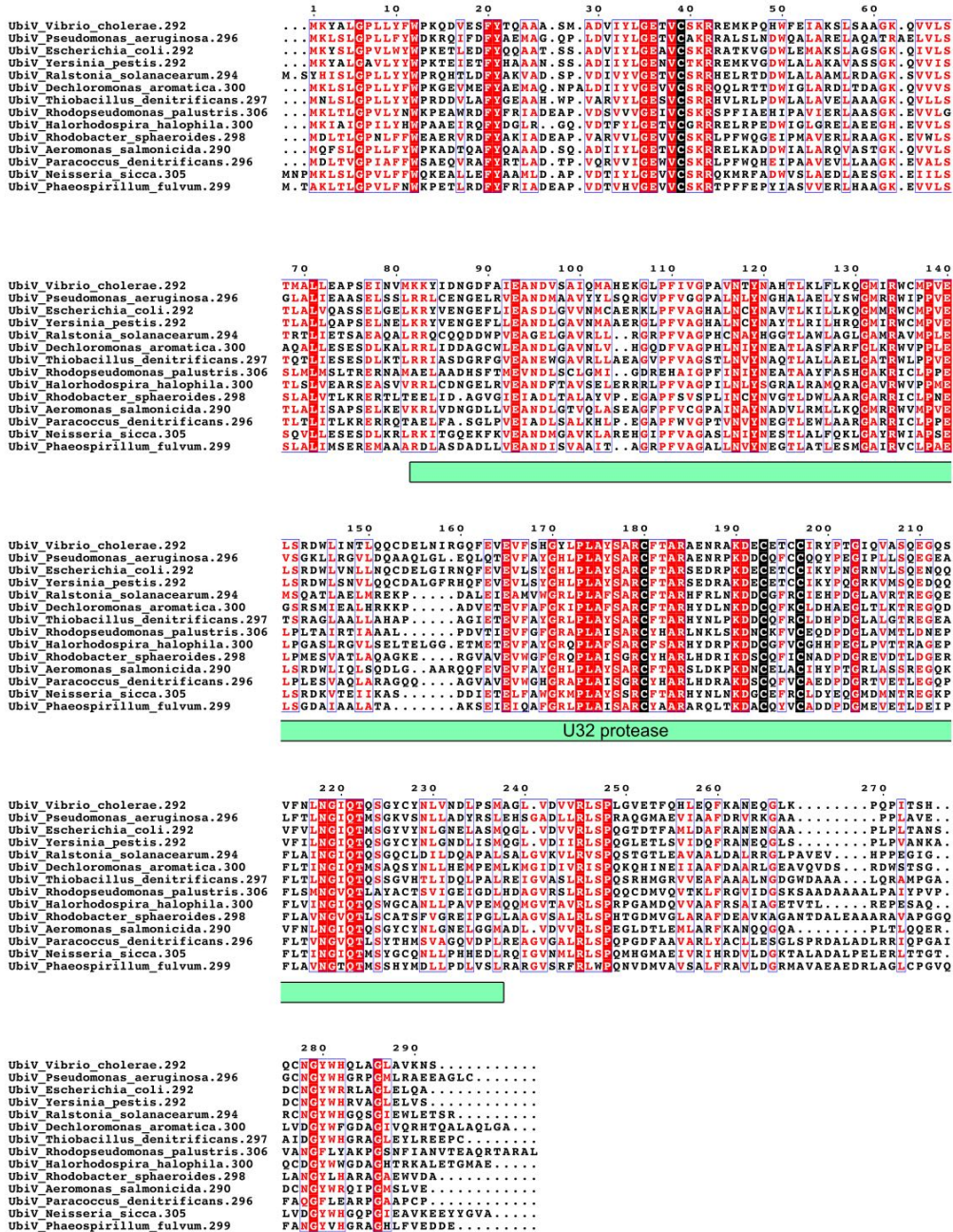
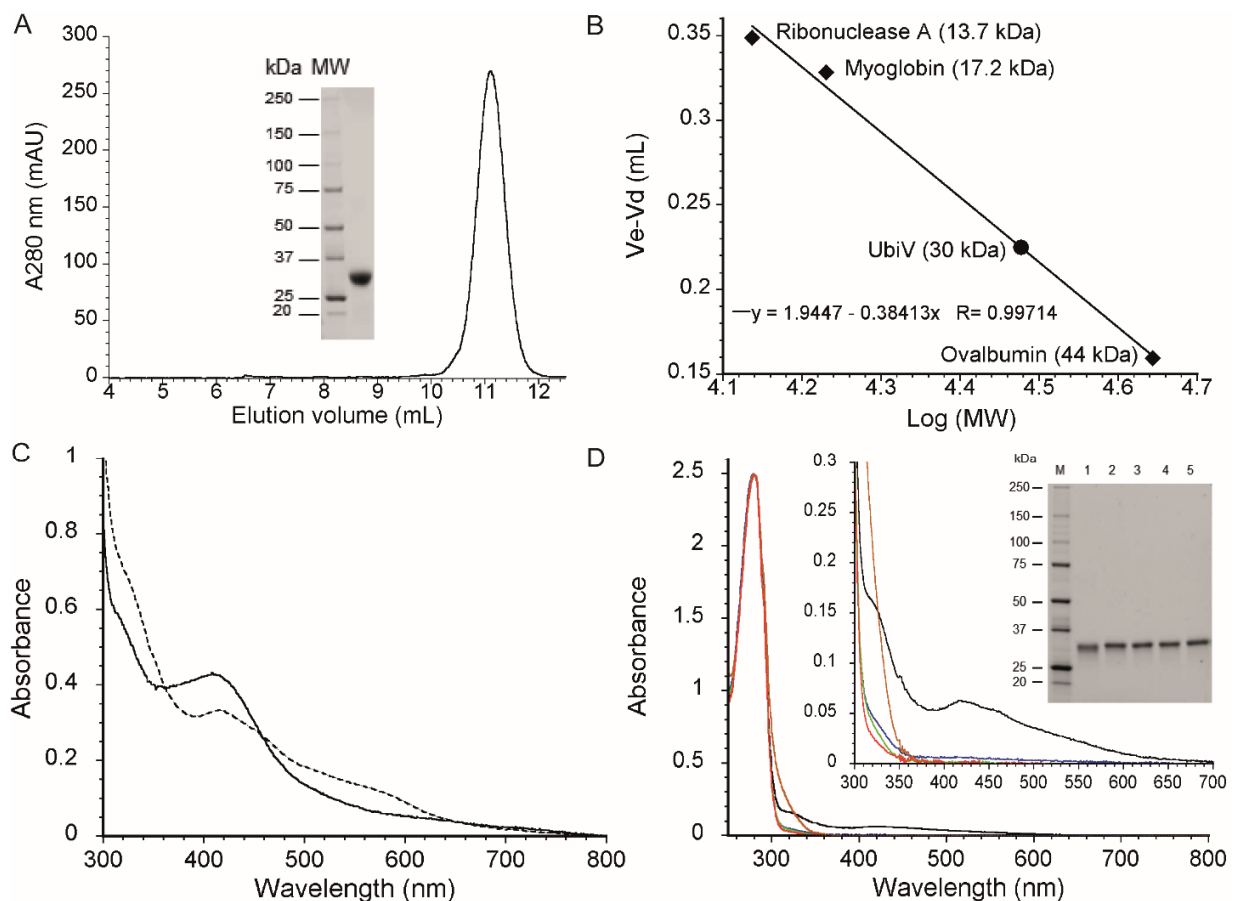


Figure S4: Multiple sequence alignment of UbiV from representative proteobacteria. Sequences were aligned using Mafft (linsi), and the output generated using ESPript and Inkscape. The four conserved cysteines (C39, C180, C193 and C197 - positions in *E. coli*) involved in iron-sulfur binding are indicated by black columns. The position of the domain U32 protease PF01136 is indicated by a green box. GenBank accession numbers: *Vibrio cholerae*, NP_230300.2, *Pseudomonas aeruginosa*, NP_252601.1, *Escherichia coli*, NP_312067.2, *Yersinia pestis*, YP_002348369.1, *Ralstonia solanacearum*, WP_011004261.1, *Dechloromonas aromaticana*, WP_011285877.1, *Thiobacillus denitrificans*, WP_011312697.1, *Rhodopseudomonas palustris*, WP_011666113.1, *Halorhodospira halophila*, WP_011813832.1, *Rhodobacter sphaeroides*, WP_011909345.1, *Aeromonas salmonicida*, WP_005310392.1, *Paracoccus denitrificans*, WP_011750458.1, *Neisseria sicca*, WP_080614296.1, *Phaeospirillum fulvum*, WP_074767477.1.



1005

1006

1007

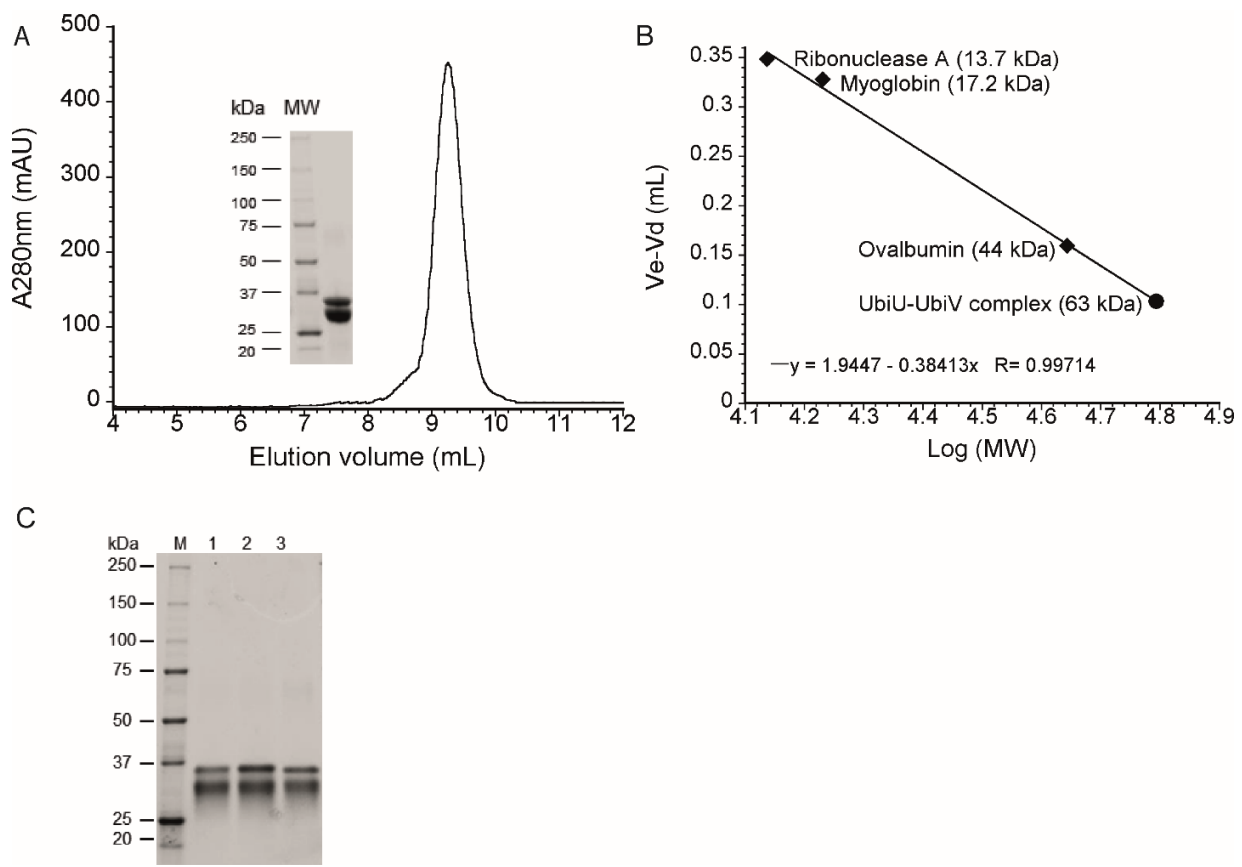
Figure S5: A) Gel filtration chromatogram of aerobically purified UbiV on a Superdex 75 Increase 10/300 GL column; Inset: Coomassie staining SDS-PAGE of aerobically purified UbiV. B) Calibration curve, standard proteins in rhombi, UbiV in circle. C) UV-visible absorption spectra of 41 μ M holo-UbiV under anaerobiosis (solid line) and after 20 minutes exposure to air (dotted line). D) Comparative UV-visible absorption spectra of aerobically purified wild-type (black) and different Cys-to-Ala mutants of UbiV (C193A C197A in blue; C39A C193A C197A in green; C180A C193A C197A in pink; C39A C180A C193A C197A in brown). Inset: Coomassie staining SDS-PAGE shows the purifications of UbiV and variants. Lanes are: M, molecular mass marker; 1, wild-type UbiV; 2, UbiV C193A C197A; 3, UbiV C39A C193A C197A; 4, UbiV C180A C193A C197A; 5, UbiV C39A C180A C193A C197. All proteins were in 50 mM Tris-HCl, pH 8.5, 25 mM NaCl, 15% glycerol, 1 mM DTT (A-D).

1017

1018

1019

1020



1023 **Figure S6:** A) Gel filtration chromatogram of aerobically purified UbiU-UbiV on a Superdex 75 Increase
1024 10/300 GL column; Inset: Coomassie staining SDS-PAGE of aerobically purified UbiU-UbiV complex. B)
1025 Calibration curve, standard proteins in rhombi, UbiU-UbiV in circle. C) Coomassie staining SDS-PAGE
1026 shows the purifications of UbiU-UbiV wild-type and variants proteins: Lanes are: M, molecular mass
1027 marker; 1, wild-type UbiU-UbiV complex; 2, UbiU C169A C176A - UbiV wild-type; 3, UbiU C193A C232A -
1028 UbiV wild-type. All proteins were in buffer 50 mM Tris-HCl, pH 8.5, 150 mM NaCl, 15% glycerol, 1 mM
1029 DTT (A-D).

1030

1031

1032

1033 **Table S1:** UQ levels in strains from the medium- and large- deletion collections

1034 **Table S2:** Occurrence of genes from the UQ pathways in bacterial genomes.

1035 **Table S3:** List of oligonucleotides and strains used in this study

1036 **Table S4:** References of the protein sequences used to build the HMM profiles.

1037